# Shear-Induced Precursor Structures in Isotactic Polypropylene Melt by in-Situ Rheo-SAXS and Rheo-WAXD Studies

**Rajesh H. Somani, Ling Yang, and Benjamin S. Hsiao***

*Department of Chemistry, State University of New York, Stony Brook, New York 11794-3400*

**Pawan K. Agarwal, Hitesh A. Fruitwala, and Andy H. Tsou**

*ExxonMobil Chemical Company, Baytown Polymers Center, Texas 77522*

*Received May 22, 2002; Revised Manuscript Received September 19, 2002*

ABSTRACT: In-situ rheo-SAXS (small-angle X-ray scattering) and rheo-WAXD (wide-angle X-ray diffraction) studies were carried out to investigate the nature of shear-induced precursor structures in isotactic polypropylene (iPP) melt at 165 °C, near its nominal melting point. Immediately upon the cessation of shear, SAXS patterns clearly showed an evolution of oriented structures in hundreds of angstroms, while the corresponding WAXD patterns did not exhibit any crystal reflections. SAXS patterns at later times showed that the shish-kebab morphology was developed, and the kebabs possessed only a small amount of crystallinity (3%). The combined SAXS and WAXD results indicate that, at the early stages of crystallization, a scaffold (network) of oriented structures is formed. These structures contain (1) primary nuclei (through homogeneous nucleation) that may be crystalline or mesomorphic but having linear connectivity along the flow direction, which form the shish entity, and (2) shish-induced layered crystalline lamellae (kebabs) oriented perpendicularly to the flow direction that have poor lateral connectivity. Subsequent polymer crystallization takes place in the framework of the scaffold, which is probably dominated by the lower molecular weight species. Amounts of the crystalline primary nuclei and the layered crystalline lamellae in the precursor structures were estimated. The results verified, quantitatively for the first time, the well-known concept that minor amounts of linear nuclei induce multiple secondary nucleation sites for the growth of a large quantity of lamellae that grow radially outward from the central core. A mechanistic pathway for the early stages of crystallization in polymer melts under flow is proposed.

## Introduction

It is well-known that during polymer processing the crystallization kinetics and the final morphology, whether it being spherulitic, cylindrite, or fibrillar, are deeply influenced by molecular orientation induced by flow (in the molten state) and deformation (in the solid state).[1−20] Understanding and quantification of these effects are extremely important from both scientific and technological basis. Many studies have been carried out to investigate the molecular orientation in the deformed melt and the resultant morphological changes during the crystallization process utilizing various combined characterization techniques. These techniques can be divided into two types: (1) the in-situ methods such as rheo-SALS (small-angle light scattering),[21−25] rheo-optical methods,[26−32] and rheo-X-ray scattering[33−41] and (2) ex-situ methods such as optical microscopy, atomic force microscopy (AFM), and transmission electron microscopy (TEM).[42−44] A brief summary of these studies is as follows. Results of time-resolved SALS and rheo-optical techniques obtained by Winter and co-workers[21−24] showed that density fluctuations occur before the development of crystalline organization which is related to nucleating events. Monasse and co-workers[25] confirmed the results obtained by Winter et al., which indicated that the local orientation of macromolecular chains rather than the average orientation is likely to dictate the flow-induced crystallization behavior. Janeschitz-Kriegl et al.[26−28] studied the growth of birefringence in polymer melts during and after intense short-term shear. The sudden rise in birefringence was explained by the formation of shear-induced linear precursors. Kornfield and co-workers[29−32] monitored the birefringence of supercooled iPP upon short-term shearing. They found that the time of the birefringence upturn was correlated with the rheological shift factor of the polymer melts. Ryan and co-workers used synchrotron X-ray scattering techniques[34,35] to study the polymer crystallization with long induction times and reported that large-scale density fluctuations occur prior to crystal growth. Alfonso et al.[45] adopted the fiber-pulling experiment to study the effect of high shear rates at high temperatures on crystallization of isotactic polybutene-1. They attributed the formation of cylindritic morphology around the pulled fiber to the generation of long-living ordered clusters that were formed by bundles of chain segments oriented along the flow direction, which acted as nucleation centers for subsequent crystallization. Their results showed that the holding time necessary to fully erase the memory of intense flow was long for high molecular weight chains. Also, those large ordered clusters survived the relaxation process after cessation of flow, where the survival time of oriented clusters depended on molecular weight and was very sensitive to temperature. Bassett and co-workers[46−48] made TEM observations of lamellae in row structures grown from their primary nuclei and have elaborated on the fundamentals of orientation-induced crystallization and the molecular mechanisms involved.

The above findings have provided many useful insights into the different stages of orientation-induced

* To whom correspondence should be addressed. E-mail: bhsiao@notes.cc.sunysb.edu.

10.1021/ma020785o CCC: $22.00 
Published on Web 10/26/2002

crystallization from an entangled polymer melt. However, the mechanisms for the earliest stages of crystallization, i.e., pathways for primary nucleation under flow, are still not well understood. Flow-induced nucleation is a homogeneous nucleation process; herein, we also term it primary nucleation, because it is initiated from a single phase (polymer melt). Perhaps the lack of understanding is due to the intrinsic difficulty in performing precise experiments at the early stages of crystallization. The nature of the primary nuclei, their spatial arrangement, and correlations essentially dictate subsequent crystallization through secondary nucleation processes (initiated from the two phases) that can lead to different morphologies. Thus, the control of the initial nuclei topology or landscape is the key to manipulate the final morphology. Recently, several researchers have proposed new concepts and schemes involving primary nuclei and their role in the initiation of crystallization under quiescent conditions. For example, Strobl[49] proposed that polymer crystallization from an entangled melt might resemble the ordering processes observed in two-dimensional systems rather than the general scheme of nucleation and growth. He suggested that the formation and growth of crystals is not a one-step process proceeding directly into the melt but follows a route over a sequence of intermediate states: an initial liquidlike packing in the mesomorphic state (which can be considered as primary nuclei in our view), followed by a state of granular crystal blocks and then the final lamellar crystals. Lotz,[50] however, has raised some critical concerns about such a scheme, pointing out crystallization of chiral but racemic polymers such as isotactic polypropylene (iPP), in which building units of the crystal are right-handed and left-handed helical stems, ~10−20 nm long. He viewed the crystallization as a highly sequential and substrate-determined process, where the depositing stem often first probes the topography of the growth face before attachment. Thus, the crystal growth mechanisms based on condensation/deposition of pseudo-crystalline precursor bundles as suggested by Strobl may not apply to all polymer systems in general. Alternatively, the spinodal-like behavior in a supercooled polymer melt and spinodal decomposition as a preliminary step in the crystallization process have been proposed by several research groups including Ryan et al.,[34,35] Kaji et al.,[51−53] Petermann et al.,[54,55] and Meakin et al.[56] The spinodal decomposition step prior to polymer crystallization has been questioned, for the reasons outlined before, by our group[57,58] as well as by others.[59−61] Muthukumar and co-workers have carried out some elegant modeling works to simulate the formation of primary nuclei under the quiescent state.[60,61] The major physical characteristics from this simulation are consistent with various experimental observations.

One of the objectives for our current research was to advance the understanding of the nature as well as to elucidate the pathway for formation of primary nuclei induced by flow prior to the events of crystallization steps dominated by secondary nucleation or the growth process. The experimental techniques used in this study were complementary methods involving synchrotron small-angle X-ray scattering (SAXS) and wide-angle X-ray diffraction (WAXD) in a parallel-plate shear apparatus. The in-situ rheo-SAXS technique gave 2D maps of density fluctuations in the reciprocal space, which allowed us to construct the superstructure of crystallization precursors induced by flow, i.e., their orientation, spacing, and relative amounts. The corresponding 2D WAXD images were used to determine the crystallinity, crystal orientation, and crystal form. As noted below in detail, the proper selection of a suitable experimental temperature turned out to be of critical importance. This is because if the test temperature is too high, no precursor structures can be detected. If the temperature is too low, the rapid crystal growth would quickly overwhelm the initial precursor structures, which has been noted in earlier studies.[39−41] In this work, we found that the experimental temperature in the vicinity of the nominal melting point 165 °C for iPP provided us the best experimental window to observe the flow-induced structures at the very early stages of crystallization.

We note that several flow studies in the supercooled polymer melts near the nominal melting point have been carried out. For example, Kornfield and co-workers[30,31] used a rheo-optical technique to study the influence of short-term shearing in the iPP melt at 175 °C. The changes in melt birefringence were monitored after cessation of shear. These measurements provided an indirect evidence of formation of the "shear-induced structures" in the melt at high temperatures. However, the optical techniques cannot elucidate the molecular information. The in-situ rheo-SAXS and rheo-WAXD techniques turn out to be powerful methods to reveal new information on the orientation-induced structures in crystallizing polymer melts. A few preliminary results of rheo-X-ray studies at high temperatures above the nominal melting point have recently been reported by our laboratory.[36−38] In one study,[36] the iPP melt was subjected to a step-shear (shear rate 60 $s^{-1}$, shear duration = 0.25 s) at 175 °C, and in other studies,[37,38] a step-shear with longer during time (shear rate 60 $s^{-1}$, shear duration = 5 s) at 165 °C was used. The imposed shear conditions were found to generate oriented structures that were stable at high temperatures, as evidenced by in-situ SAXS patterns obtained after shear, where no detectable WAXD crystalline reflections were seen. These results provided new insight into the morphological features of a layered superstructure induced by flow prior to crystallization as well as laid the ground wok for the study reported here.

In this work, the same iPP polymer has been studied by in-situ rheo-SAXS and -WAXD techniques under two different shearing conditions: (1) a relatively weak shear (shear duration ($t_s$) = 0.25 s) and (2) a stronger shear (20 times longer duration time, $t_s$ = 5 s)—both at the temperature of 165 °C and the shear rate of 60 $s^{-1}$. The chosen experimental conditions of temperature and shear offered us a unique opportunity to follow the development of flow-induced structures at the very early stages of crystallization in real time. A deconvolution procedure[39,59] was used to extract the fraction of the scattered intensity due to the oriented structures (parallel and perpendicular to the flow direction) from the 2D SAXS data. The volume fractions of the shish (microfibril) and the kebab (layered lamellae) were determined from their relative contributions to the total SAXS intensity. The crystallinity values were obtained from the corresponding WAXD data. Our results do not suggest any deviations from the classical nucleation and growth concepts for polymer crystallization during flow. Instead, we present here a mechanistic model for the development of primary nuclei by molecular orientation

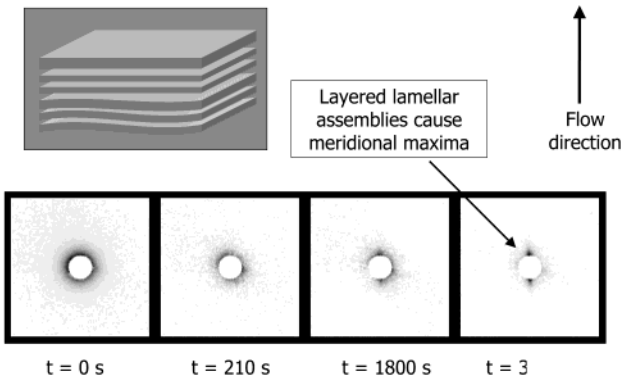


**Figure 1.** 2D SAXS patterns of iPP melt before and at selected times after shear (shear rate = 60 $s^{-1}$, $t_s$ = 0.25 s, $T$ = 165 °C).

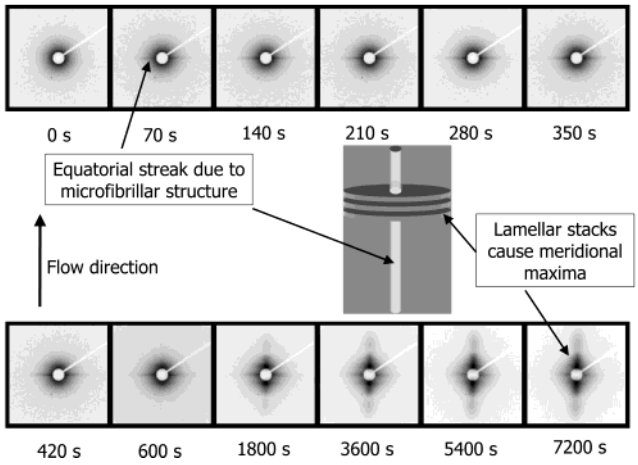


**Figure 2.** 2D SAXS patterns of iPP melt before and at selected times after shear (shear rate = 60 $s^{-1}$, $t_s$ = 5 s, $T$ = 165 °C).

during flow and possible pathways for subsequent crystallization processses from these nuclei.

## Experimental Section

A Ziegler−Natta iPP homopolymer supplied by ExxonMobil Chemical Co. was used in this study. Its molecular weights were $M_n$ = 92 000 g/mol, $M_w$ = 368 000 g/mol, and $M_z$ = 965 000 g/mol. In-situ rheo-SAXS and -WAXD measurements were carried out in the beamlines X27C and X3A2, respectively, at the National Synchrotron Light Source (NSLS), Brookhaven National Laboratory (BNL). A 2D MAR CCD X-ray detector (MARUSA) was employed to collect time-resolved SAXS and WAXD patterns in the shear experiments. The details of the Linkam shear apparatus and synchrotron X-ray experimental procedures have been described in previous publications.[39−41] The temperature protocol for shear experiments was as follows: (a) heat the polymer sample from room temperature to 200 °C at a rate of 30 °C/min, (b) hold the temperature at 200 °C for 1200 s, (c) cool at a rate of 30 °C/min down to 165 °C, and (d) hold the temperature at 165 °C for X-ray measurements.

The polymer melt was subjected to shear immediately after the temperature dropped to 165 °C. A shear rate of 60 $s^{-1}$ and two shear durations, $t_s$ = 0.25 and 5 s, were selected. Two-dimensional patterns (SAXS or WAXD) were collected continuously: before, during, and after cessation of shear. All X-ray images were corrected by sample absorption and beam fluctuation.

## Results

**Rheo-SAXS.** Figures 1 and 2 show selected SAXS patterns (the flow direction is vertical) of the iPP melt at different times after shear under two chosen conditions of shear, $t_s$ = 0.25 and 5 s, respectively. Two scattering maxima along the shear direction are seen in SAXS patterns at times longer than 1800 s for shear condition of $t_s$ = 0.25 s (Figure 1). The meridional maxima in the SAXS patterns can be attributed to the evolution of kebab-like lamellar structures that are correlated and oriented perpendicular to the flow direction, as shown in the schematic diagram. (Here we used the terminology of meridian and equator to indicate that the induced structures have a fiber symmetry.) However, no equatorial streak is observed at either early or later stages for shear condition of $t_s$ = 0.25 s. This is very similar to our previous study of the same polymer at a higher temperature 175 °C.[36] On the other hand, the SAXS patterns obtained for shear condition of $t_s$ = 5 s (Figure 2) clearly show the emergence of an equatorial streak immediately after shear (pattern at $t$ = 70 s). The streak becomes stronger with increasing time as evident from SAXS images taken at subsequent time intervals ($t$ > 140 s). The equatorial streak can be attributed to the formation of microfibrils, bundles of parallel chains consisting of either mesophase or crystalline entities parallel to the flow direction in the schematic diagram in Figure 2. Note that a collection of noncorrelated shish structures (microfibrils) can give rise to the equatorial streak in SAXS patterns. Also, it can arise from isolated, narrow shish-kebab entities that can form in a short time period after shear. The meridional maxima emerge after the development of equatorial streak, as can be seen in the SAXS patterns at later times: $t$ = 600, 1200, and 7200 s (Figure 2).

The SAXS patterns obtained for shear condition of $t_s$ = 5 s verfy the shish-kebab morphology at the initial stages of flow-induced crystallization in polymer melt. (Though the qualtitative aspects of this behavior have been conjectured and presented by Schultz, Hsiao, and co-workers[62,63] in in-situ X-ray studies of fiber spinning, to our knowledge, quantification of the experimental observations has never been made.) In other words, our observation confirms the formation of extended linear nuclei parallel to the flow direction by primay nucleation that are large enough to be detected by SAXS. From these nuclei, lamellae grow epitaxially and radially via the secondary nucleation process. The missing equatorial streak in the SAXS patterns for shear condition of $t_s$ = 0.25 s indicates that the melt consists of kebab-like structures only. However, if the linear nuclei were not formed, then what causes the nucleation and growth of stacks of lamella oriented perpendicular to flow direction? One possibility is that the missing equatorial streak under weak conditions of shear is probably due to the low concentration of the shish structures; also possible is the fact that the shish structures are too small that they are beyond the detection limits of our SAXS setup. Another explanation, previously suggested by Schultz et al.,[63] for the missing equatorial streak is that as kebab-like structures grow from the shish, the rodlike scatterer becomes "cylindrical"-like. As this cylinder grows radially, its scattering converges toward the origin and finally disappears. Under stronger conditions of shear ($t_s$ = 5 s), it is expected that the concentration of shish would be higher and the shish diameter may be bigger, which allow an easy detection of SAXS.

**Rheo-WAXD.** Typically, under shear, iPP can crystallize into a stable α-form exhibiting five distinct

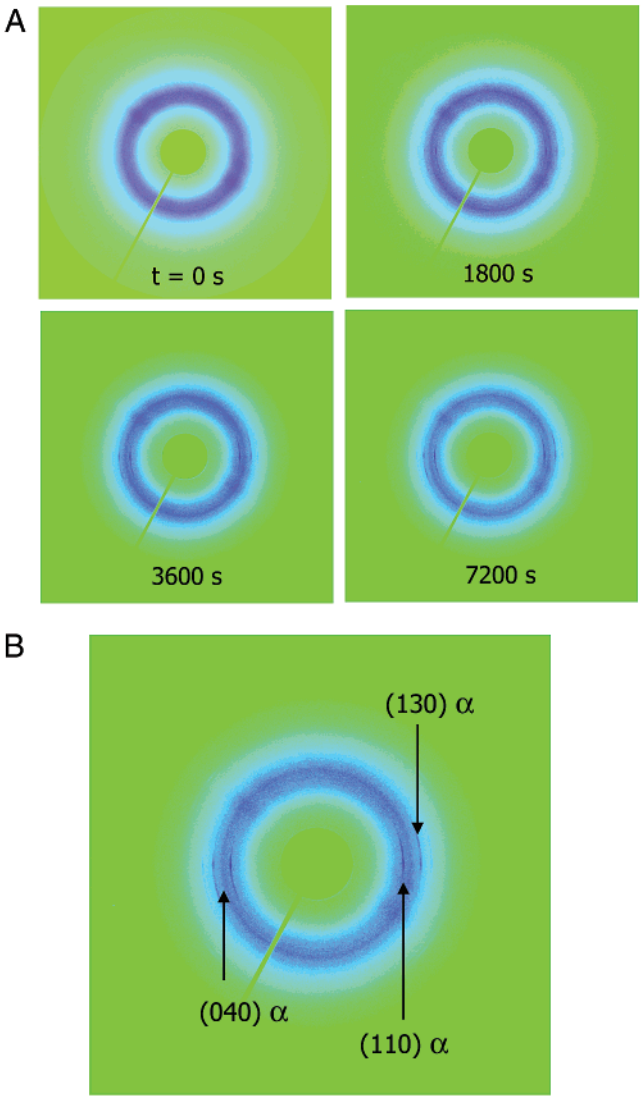


**Figure 3.** 2D WAXD patterns of (A) iPP melt before and at selected times after shear (shear rate = 60 $s^{-1}$, $t_s$ = 5 s, $T$ = 165 °C) and (B) at $t$ = 7200 s after shear (the equatorial peaks were indexed by the α-crystal form).

reflections in the WAXD pattern: (110) at $2\theta = 14.1°$, (040) at 16.9°, (130) at 18.5°, (111) at 21.4°, and (−131) at 21.8°.[41] Figure 3a shows in-situ rheo-WAXD patterns of iPP melt obtained at the stronger shear condition ($T$ = 165 °C, shear rate = 60 $s^{-1}$, $t_s$ = 5 s). (We note that no crystal reflections were observed in the WAXD patterns obtained for the weaker shear conditions ($t_s$ = 0.25 s).) Even in the WAXD patterns obtained under stronger conditions of shear, only three weak reflections [(110), (040), and (130)] of iPP α-form all along the equator are observed and that also at much later times after the cessation of the shear (Figure 3b). These three reflections are sharp and have narrow azimuthal width, which indicates a highly oriented nature of iPP crystals with good crystalline resgistration. The volume fraction of the oriented crystals and the corresponding crystallinity from the shish-kebab structures were obtained using the following procedures.

**Analysis of SAXS and WAXD Data.** The SAXS patterns obtained at the later stages after cessation of shear ($t$ > 600 s, Figure 2) show the development of shish-kebab morphology in the sheared iPP melt; the corresponding WAXD patterns (Figure 3) indicate that these flow-induced structures are at least partially

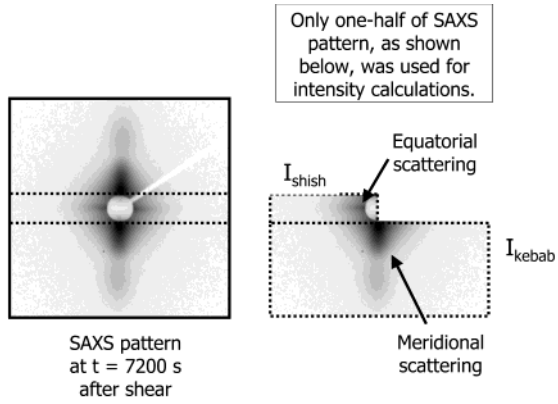


**Figure 4.** Sections of 2D SAXS pattern for calculation of the integrated SAXS intensity due to shish ($I_{shish}$) and kebab ($I_{kebab}$) structures.

crystalline. While the SAXS patterns at the initial stages (immediately after shear) show emergence of shish followed by kebab-like structures, the corresponding WAXD patterns do not exhibit any crystalline reflections. However, this does not suggest that the shish structure is not crystalline. It is possible that its crystallinity is below the detection limit of WAXD (1%).[57] The SAXS and WAXD data were thus further analyzed to reveal the nature of the oriented structures in polymer melt after shear.

**Time Evolution of Shish-Kebab Structures by SAXS.** As pointed out in our earlier study[39] that the total integrated scattered intensity of each SAXS pattern, $I_{total}$, can be deconvoluted into two components: (1) $I_{isotropic}$, which is due to scattering from the randomly distributed scatterers (it arises primarily from the amorphous polymer melt at high temperatures), and (2) $I_{oriented}$, originated by scattering from the correlated oriented structures in the polymer melt (note here that we avoid using the word crystallites, since oriented structures formed at the initial stages may not be totally crystalline). The scattered intensity arising from the unoriented scatterers (isotropic) is azimuthal independent (thus a function of $s$ only, where $s$ is the scattering vector = 2 sin $\theta/\lambda$, with $2\theta$ being the scattering angle), whereas the scattering arising from the oriented scatterers is azimuthal dependent (function of $s$ and $\phi$, where $\phi$ is the azimuthal angle). Our analysis indicates that the contribution of $I_{isotropic}$ is very low (<5%) in the SAXS patterns for both shear conditions, suggesting that the flow-induced structures during the experimental time frame are highly oriented.

We have also applied an alternate procedure to deconvolute the contributions of oriented SAXS intensity of the shish ($I_{shish}$) and kebab fractions ($I_{kebab}$) by sectioning the oriented SAXS pattern, i.e., after the "Halo" subtraction to eliminate the unoriented component.[64] Figure 4 shows two sections of a 2D SAXS pattern ($t_s$ = 5 s), which have been used for calculation of $I_{shish}$ and $I_{kebab}$. Time evolution of intensities $I_{shish}$ and $I_{kebab}$ calculated by this method at selected times after shear are illustrated in Figure 5. It is seen that $I_{shish}$ rises immediately after shear (Figure 5a), while $I_{kebab}$ increases only after a short induction time, about 210 s (see inset of Figure 5b). Although $I_{shish}$ rises rapidly immediately at initial times, its rate of increase diminishes at the later times. On the other hand, $I_{kebab}$ increases at a much greater rate than $I_{shish}$. It reaches a significantly higher value, about 24 times higher than

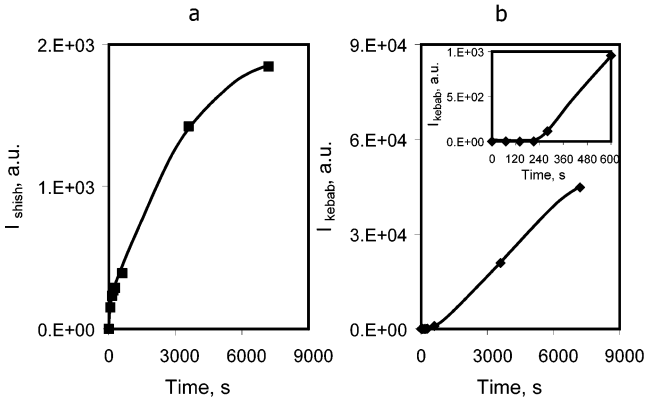


**Figure 5.** Time evolution of SAXS integrated intensities: (A) $I_{shish}$ and (B) $I_{kebab}$ after shear (shear rate = 60 $s^{-1}$, $t_s$ = 5 s, $T$ = 165 °C).

$I_{shish}$ at $t$ = 7200 s after shear. The interpretations of these observations are as follows.

Immediately after shear, the emergence of the shish structures in the amorphous melt results in a rapid jump in $I_{shish}$. This initial increase in the shish fraction is due to the formation of extended chain bundles (nuclei) with favored thermodynamic driving forces (i.e., a lower Gibbs free energy). However, as the shear stops, the relaxation of polymer chains will also begin immediately, which hinders the formation of additional nuclei (or bundles). Motions of the polymer segments in the shish structures (microfibrils) are not completely restricted because the segments may not be locked in an ordered crystalline struture as yet. The rise in $I_{shish}$ can be attributed to the further ordering of the chains in the shish structures (that results in the increase of electron density contrast) as well as their growth along the flow direction after cessation of flow (that results in the increase of the shish volume). These observations are consistent with the results of a recent study by Petermann et al.,[65] who concluded that the shish crystal growth can be an autocatalytic process. That process can induce a self-orientation of the molecules in the growth front of the crystal tip and does not necessarily require an external flow field. Thus, as polymer molecules in the melt relax, the rise in $I_{shish}$ is low as it is only due to the process of forming ordered extended chain crystals along the flow direction. The increase in $I_{shish}$ also implies that the connectivity between the linear nuclei along the flow direction can significantly increase with time.

After the formation of the shish structure, oriented crystals are initiated from the linear nuclei and grow perpendicularly to the flow direction forming layered lamellar structures. This is seen by the emergence of meridional maxima in the SAXS patterns after a short time delay. The nature of these lamellar structures is crystalline, but its mass fraction may be limited as noted by the weak contribution of crystal diffraction peaks in WAXD. Despite its low crystallinity, the increase in $I_{kebab}$ (Figure 5b) is found to be much greater than that in $I_{shish}$ at the later stages.

**Time of Kebab Emergence after Shear.** To determine the exact time of the emergence of meridional maxima (arises from the kebab structures) after the stronger shear ($t_s$ = 5 s), Lorentz-corrected 1D SAXS intensity profiles ($Iq^2$ vs $q$) along the shear direction were calculated from the 2D SAXS images at selected times. These are shown in Figure 6. The meridional

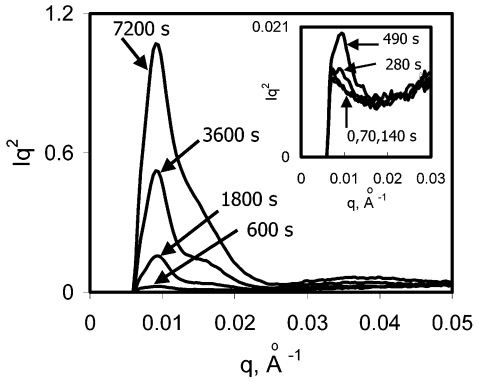


**Figure 6.** Lorentz-corrected SAXS intensity profiles along the meridian. The inset shows profiles (magnified) at the early stages after shear (shear rate = 60 $s^{-1}$, $t_s$ = 5 s, $T$ = 165 °C).

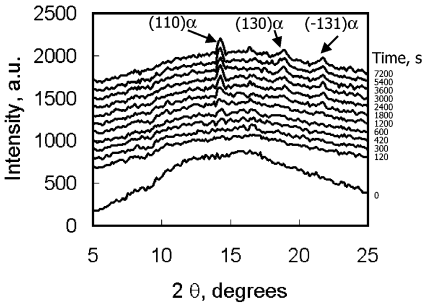


**Figure 7.** 1D WAXD intensity profiles along the equator at selected times after shear (shear rate = 60 $s^{-1}$, $t_s$ = 5 s, $T$ = 165 °C).

intensity maximum (peak) can be clearly seen in these profiles; the magnified SAXS intensity profiles at the early stages are shown in the inset of Figure 6. The meridional maximum is first observed at $t$ = 280 s after shear, which is consistent with the onset point of the SAXS integrated intensity ($I_{kebab}$) profile in Figure 5b. The spacing between the adjacent lamellar stacks is estimated to be about 600 Å. Typically, the long spacing in fully crystallized iPP solid is in the range 200−300 Å; the large spacing between the layers is an indication of a loosely packed lamellar structures at the early stages of crystallization.

**Crystallinity Development by WAXD.** Figure 7 shows the linear WAXD intensity profiles taken from the equatorial slice of the 2D WAXD patterns at selected times after shear, where the α-crystal reflection signals are the strongest. The (110) reflection of the α-crystals is observed only about 600 s after shear. The mass fraction of crystallites in the melt can be estimated by standard peak-fitting procedure of the integrated WAXD intensity profile (not of the equatorial profile). Note that the crystal reflection signals are very weak, particularly at the beginning of the process. Only a few selected profiles at later times can be analyzed by the curve-fitting method with a fair degree of accuracy. The percent crystallinity was estimated by subtracting the area under the fitted profile of the amorphous halo from the total area, and the result is shown in Figure 8. It is seen that even at $t$ = 7200 s after shear, the measured crystallinity is only about 2.3%. Such a low crystallinity can be attributed to two reasons: (1) the chosen temperature (165 °C) is near the nominal melting point of typical iPP crystals, and (2) only the shear-induced oriented crystals that are stable at such a high melt temperature can contribute to the crystallinity. At $t$ = 7200 s after shear, while a very small fraction of

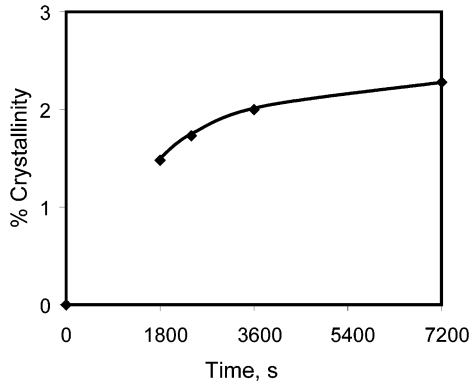


**Figure 8.** Development of crystallinity in iPP melt at selected times after shear (shear rate = 60 $s^{-1}$, $t_s$ = 5 s, $T$ = 165 °C).

isotropic crystals may be stable above the nominal melting point, both SAXS and WAXD results suggest that the melt consists mostly of oriented crystals. Thus, the calculated crystallinity can be viewed as the oriented crystal fraction in iPP melt at 165 °C.

**Estimates of Fractions for Shish and Kebab Crystals.** The mass fractions of crystals in shish and kebab structures, $X_{shish}$ and $X_{kebab}$, can be estimated from (1) the measured crystallinity $X_c$ by WAXD and (2) the ratio of SAXS intensity between the shish ($I_{shish}$) and kebab structures ($I_{kebab}$). If we assume that the SAXS intensity is directly proportional to the amount of crystallinity, which is reasonable at the initial stages of crystallization,[57] the following relationships for $X_{shish}$ and $X_{kebab}$ can be written in terms of the results obtained from the SAXS and WAXD data.

$$X_{shish} + X_{kebab} = X_c \quad \text{(WAXD)} \tag{1}$$

$$X_{kebab}/X_{shish} = I_{kebab}/I_{shish} \quad \text{(SAXS)} \tag{2}$$

The mass fraction of the total oriented crystals, $X_c$, at $t$ = 7200 s after shear as estimated from WAXD is 2.3%, and the corresponding value of $I_{kebab}/I_{shish}$ ratio from SAXS is 24. Thus, at $t$ = 7200 s after shear, the values of $X_{shish}$ and $X_{kebab}$ in the iPP melt at 165 °C are 0.1% and 2.2%, respectively. Although the calculated value of $X_{shish}$ is too low to be statistically meaningful, the order of magnitude must be correct. It is clear that only a very small fraction of crystalline structure exists in the shish. The kebabs later developed have a much higher crystallinity.

## Discussion

As mentioned earlier, in recent years, various groups have proposed novel schemes for polymer crystallization under quiescent conditions that are notably different from the conventional nucleation and growth pathways. On the basis of this and our previous studies, we present here our current views on the pathways of crystallization in polymer melts under flow, especially those contemplated to take place at the very early stages of crystallization.

**Formation of Shish Structures Containing Primary Nuclei.** Obviously, the first effect of the applied shear (or any external field) is the orientation of chain segments in the direction of the flow. The applied shear (conditions) would dictate the extent of molecular orientation. The aggregation of oriented chain segments may take place in the following fashion. In short-term shear experiments, such as of the present study, after the cessation of shear, oriented chain segments begin to relax according to the relaxation behavior that scales with weight-average molecular weight as $M$.[3,4] Thus, the oriented chain segments of the low molecular weight molecules will relax to the random state rapidly, and the oriented chain segments of high molecular weight molecules can remain oriented for a long period.[29,66] It is reasonable to expect that only a fraction of the chain can stay oriented in the flow direction and the rest of the chain, especially the segments near the chain ends, cannot easily retain orientation. Aggregation of oriented chain segments from different molecules that are sufficiently close distance will increase the segmental interactions and result in a cluster, especially when the diffusive interaction forces are strong.[60] Initially, a tiny cluster consisting of only a few chain segments is expected to form; the oriented tiny clusters either can grow in size by addition of new chain segments and become stable or will disappear (relax) into the unoriented melt matrix. Since only chain segments with high degree of orientation and long relaxation time can remain oriented for a longer time, it is expected that the clusters having high degrees of orientation will grow in size and form a stable structure. This structure can be considered as a primary nucleus. This nucleation process can also be termed homogeneous nucleation, since it is evolved from a single phase of the homogeneous polymer melt.

Many nuclei in tens of angstroms can rapidly grow and forge connectivity along the flow direction to imprint the stress field. The linear assembly of multiple nuclei become the shish structure observed as the equatorial streak in SAXS, which is seen immediately upon the cessation of shear. We believe that the primary nuclei must consist of both crystalline and mesomorphic entities because the estimated crystallinity is extremely low even at 7200 s after shear ($X_{shish} \sim 0.1\%$ only). The view that polymer crystallization can be initiated from the mesomorphic phase has recently been presented by Strobl,[49] although we feel that the situation is slightly different here. To form α-monoclinic crystals in primary nuclei, the iPP chains with three chain helical conformations must be organized in a specific spatial arrangement.[50] This may not be easily accommodated during the initial stage of nuclei formation. As a result, the oriented chain segments in the nuclei may not have the correct helical registrations to form crystals. Nonetheless, they can form a thermally stable mesomorphic structure. Also, noted here are the results of Petermann et al.,[65] who showed that the shish crystal growth is an autocatalytic process which induces a self-orientation process of the molecules in the growth front even without the external flow field. Our SAXS results are in accord with their observations. Thus, after cessation of flow, the increase in the intensity of the equatorial streak can be attributed to the growth of the shish structures along the flow direction by processes of alignment and ordering of polymer chains.

The above discussion suggests that the linear structures primarily consist of oriented long chains from higher molecular weight fraction. They form the basis of primary nuclei. This argument is certainly consistent with the results of Monasse et al.[25] and Alfonso et al.[45] However; it differs from the model of threadlike precursors, recently presented by Kornfield and co-workers.[66] They argued that the mechanism of formation of point-like precursors does not preferntially involve the most

oriented chains in the melt due to long chains. The long chains only enhance previously formed pointlike precursors into threads. In this scheme, the threadlike structure is formed as a string of pointlike precursors along the line of flow. Our SAXS results do not support this representation. If the threadlike structure consists of correlated pointlike nuclei with higher electron density, excess scattering or even scattering maximum should have developed in the meridional direction of SAXS. The structural evolution base on the Kornfield model should result in the occurrence of the scattered inetsity along the meridian before or simutaneously with the appearance of equatorial streak, which is not supported by our observations. In this study, the SAXS patterns of iPP (melt at 165 °C) obtained immediately after shear clearly indicated that the equatorial streak form first and the meridional maxima emerge afterward.

**Formation of Row-Nucleated Lamellar Layers.** Growth of meridional maxima were observed in SAXS patterns after a short time delay ($t$ > 280 s, Figure 2). The meridional maxima suggest the emergence of oriented structures arranged perpendicular to the flow direction. These structures are presumed to grow epitaxially (through secondary nucleation) from the shish structure and form stable lamellar layers (kebabs). There is no doubt that these layered structures are crystalline and probably consist of folded chain crystals. The increase in the scattered intensity in the meridional direction indicates that (1) the lamellae grow larger with time and/or (2) more lamellae are nucleated. We favor condition 1 as we did not observe a long period decrease from the time sequence of the meridional maxima. (In contrast, a long period increase was seen earlier.[36]) However, we believe the lateral dimensions of these lamellae cannot be too large because of the low crystallinity that is observed. This in turn implies that the kebabs are short, and they do not form connectivity in the lateral direction. The limited crystallinity can be explained by the competition between the stability of the ordered crystalline structures and the thermal motions of molten chains at the temperature of 165 °C. Although such short lamellar structures cannot grow further (at high temperatures), they will serve as ideal nucleating sites for formation of folded chain crystals once the sample is cooled to lower temperatures.

**Scaffold of Precursor Structures Prior to Full-Scale Crystallization.** Initial SAXS and WAXD patterns suggest that a scaffold or network of precursor structures form at the early stages of crystallization by flow. This scaffold contains the shish structure with a linear assembly of primary nuclei having excellent connectivity along the flow direction and the kebab structure with folded chain lamellae having poor lateral connectivity. This semiconnected network is consistent with the recent rheo-optic results obtained by Winter et al.,[21−24] Monasse et al.,[25] Kornfield et al.,[29−32] and Alfonso et al.[45] The appearance of SAXS before WAXD has been observed before,[34,35,51−53] and there can be several reasons for a late emergence of crystal reflections observed in the rheo-WAXD experiment (Figure 3) under the same conditions of shear than the distinct appearance of SAXS (Figure 2). (1) The detection limit of WAXD is about 1 order of magnitude poorer than that of SAXS. Thus, WAXD is not capable of detecting the low crystallinity during initial crystallization.[57,58] (2) The initial crystalline ordering is too defective. (3) The flow-induced shish structures consist of a large fraction of mesophase. (4) Periodic axial density variations exist within the shish. This hypothesis is based on the observation of periodic variations in structure along the axis of the fibrillar core crystal, which was made by Rau et al.[68] It is possible that the dense regions along the precursor shish give rise to the periodic lamellae. Nevertheless, since the difference in the time of emergence of oriented structures as observed by SAXS—the equatorial streak occurs immediately after shear and the meridional maxima begins at $t \sim 280$ s—and the first appearance of crystal reflection in WAXD (at $t \sim 600$ s) is significantly large, we believe that all four factors have validity. Thus, initial SAXS patterns of the iPP melt at 165 °C after shear give an untainted view of the precusor superstructure induced by flow, before the occurrence of a full-scale crystallization that may eventually overwhelm the initial scaffold morphology. We further believe that the subsequent crystallization process is dominated by the lower molecular weight species.

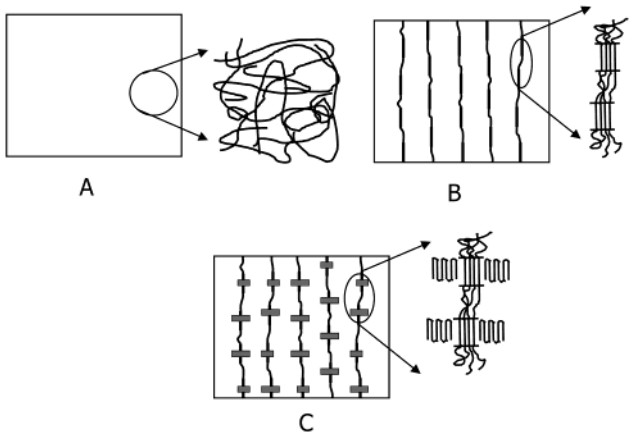


**Figure 9.** Schematic representation of flow-induced precursor structures at different stages: (A) before shear, (B) formation of precursor structures containing linear nuclei (shish), (C) formation of shish-kebab morphology through secondary nucleation from the primary nuclei.

**Proposed Mechanism for Flow-Induced Precursor Structures.** A model for the structure of polymer nuclei at the early stages of crystallization in polymer melt under flow conditions is schematically presented in Figure 9. Diagram A represents the polymer melt before shear, where molecules are in the "random coil" state. Diagram B illustrates the melt structure immediately after shear. We follow the schematic representation of the polymer orientation process and the primary nuclei growth by Petermann et al.[65] The applied flow condition immediately produces bundles of parallel chain fragments, which become thermodynamically stable, forming primary nuclei (crystalline or mesomorphic). The primary nuclei can grow along the flow direction as proposed by Petermann et al. The growth process can be maintained or enforced by a self-induced orientation of the molecules in front of the growing tip. The growth process is continued by the diffusion of new chain segments from the relaxed melt, which leads to orientation and assembly of the segments at the tip following an autocatalytic process. These segments can come from any adjacent chains with both long and short chain lengths. If the growth rate of the tip is too slow with respect to the relaxation of the chain, both sides of the assembled segments can be absorbed into the surrounding melt, which eventually destroys the local orientation field and stops the growth process.

In another scenario, if a chain is incorporated in two adjacent growth fronts, the restraints such as entanglements or branching can also stop the growth process. We envision that as the adjacent nuclei grow, they are bound to be connected by some long chains, producing a large local stress distribution in the amorphous chains surrounding the nuclei. These nuclei may be rearranged into a linear array (we term the shish structure) in order to minimize the stress concentration as seen in diagram B. This is consistent with the observations of equatorial streak (a result of uncorrelated array of the shish structures) in SAXS patterns immediately after shear. After cessation of shear, the rise in $I_{shish}$ can be attributed to the growth process of primary nuclei. Our SAXS results support the long-standing hypothesis that the shish structures exist in the polymer melt under flow, which has been argued for several decades by Keller et al.,[1] Petermann et al.,[65] and Pennings et al.[67]

Primary nuclei in the shish structures provide nucleation sites for the lateral growth of folded chain α-form crystals in iPP. The process is favored since the bundles of chain segments (primary nuclei) can also alleviate the local stress of the surrounding chains by facilitating the chain folding process through secondary nucleation. Again, we argue that the deposited chains can be of either lower molecular weight species with greater mobility or high molecular weight species with prevailing chain connection. The chain-folded crystals grow perpendicular to the flow direction and form lamellae of critical dimensions (kebabs) (diagram C). This is consistent with the SAXS observation that a scattering maximum emerges along the flow direction after a short time ($t \sim 280$ s) and grows with time. The crystal reflection signals could only be detected in the corresponding WAXD pattern at 600 s after shear. The fast rise in the SAXS intensity ($I_{kebab}$) may be due to the large density contrast between the lamellar crystals and the surrounding melt. As the crystallinity is low even at later times after shear, the connectivity between the kebabs in the initial stages is probably low. We believe, with the decrease of temperature, the subsequent crystallization process will be dominated by the rapid chain-folding crystallization of the lower molecular weight species from the existing lamellar surface. The topology of the initial crystalline lamellae such as density and orientation will dictate the morphology of the final product.

## Conclusions

In-situ SAXS and WAXD studies of sheared iPP melt at high temperature (near its nominal melting point) provide new insights into the shear-induced precursor structures at the early stages of crystallization. Our results showed that a space-filling scaffold or network, consisting of a linear assembly of primary nuclei (bundles of oriented chains) in the flow direction with good connectivity and layers of short folded-chain crystalline lamellae oriented perpendicular to the flow direction with poor lateral connectivity, is formed in the melt prior to the occurrence of full-scale crystallization. In-situ SAXS and WAXD results verified quantitatively for the first time the qualitatively known concept of the shish-kebab morphology. Our results favor the pathways of nucleation and growth for polymer crystallization under flow. Some new insights into the flow-induced precursor structures at the early stages of crystallization have been obtained: (1) formation of a stable shish structure containing a linear assembly of primary nuclei (the nuclei are mostly mesomorphic with only a small crystalline fraction), (2) formation of folded chain crystalline lamellar structures (kebabs) initiated from the primary nuclei, and (3) subsequent melt crystallization at lower temperatures is probably dominated by the lateral growth (via secondary nucleation) of lower molecular weight species from the surface of the precursor lamellae.

**Acknowledgment.** We acknowledge the assistance of Drs. Fengji Yeh, L. Liu, Dufei Fang, and S. Ran for the synchrotron SAXS and WAXD experimental setup. The critical comments by Dr. Jerold Schultz are greatly appreciated. The financial support of this work was provided by the NSF (DMR-0098104) and ExxonMobil Co. The synchrotron beam line X27C was supported by Department of Energy (DEFG02-99ER 45760).

## References and Notes

(1) Keller, A.; Kolnaar, H. W. *Mater. Sci. Technol.* **1997**, *18*, 189.
(2) Eder, G.; Janeschitz-Kriegl, H. *Mater. Sci. Technol.* **1997**, *18*, 268.
(3) Wunderlich, B. *Macromolecular Physics*; Academic: New York, 1973; Vol. 2.
(4) Keller, A.; Hikosaka, M.; Rastogi, S. *Phys. Sci.* **1996**, *T66*, 243.
(5) Keller, A.; Hikosaka, M.; Rastogi, S.; Toda, A.; Barham, P. J.; Goldbeck-Wood, G. *J. Mater. Sci.* **1994**, *29*, 2579.
(6) Keller, A.; Cheng, S. Z. D. *Polymer* **1998**, *39*, 4461.
(7) Pennings, A. J.; Van der Mark, J. M. A.; Booij, H. C. *Kolloid Z. Z. Polym.* **1970**, *236*, 99.
(8) Mackley, M. R.; Keller, A. *Polymer* **1973**, *14*, 16.
(9) Pope, D. P.; Keller, A. *Colloid Polym. Sci.* **1978**, *256*, 751.
(10) Miles, M. J.; Keller, A. *Polymer* **1980**, *21*, 1295.
(11) Bayer, R. K.; Eliah, A. E.; Seferis, J. C. *Polym. Eng. Rev.* **1984**, *4*, 201.
(12) Ania, F.; Bayer, R. K.; Tschmel, A.; Michler, H. G.; Naumann, I.; Baltá Calleja, F. J. *J. Mater. Sci.* **1996**, *31*, 4199.
(13) Rueda, D. R.; Ania, F.; Baltá Calleja, F. J. *Polymer* **1997**, *38*, 2027.
(14) Kalay, G.; Bevis, M. J. *J. Polym. Sci., Polym. Phys.* **1997**, *35*, 265.
(15) Wilkinson, A. N.; Ryan, A. J. *Polymer Processing and Structure Development*; Kluwer: Dordrecht, 1998.
(16) Varga, J. *J. Mater. Sci.* **1992**, *27*, 2557.
(17) Varga, J.; Karger-Kocsis, J. *J. Polym. Sci., Part B: Polym. Phys.* **1996**, *34*, 657.
(18) Vleeshouwers, S.; Meijer, H. E. H. *Rheol. Acta* **1996**, *35*, 391.
(19) White, H. M.; Bassett, D. C. *Polymer* **1997**, *38*, 5515.
(20) Goschel, U.; Swartjes, F. H. M.; Peters, G.. W. M.; Meijer, H. E. H. *Polymer* **2000**, *41*, 1541.
(21) Pogodina, N. V.; Lavrenko, V. P.; Winter, H. H.; Srinivas, S. *Polymer* **2001**, *42*, 9031.
(22) Pogodina, N. V.; Winter, H. H.; Srinivas, S. *J. Polym. Sci., Part B: Polym. Phys.* **1999**, *37*, 3512.
(23) Pogodina, N. V.; Soddiquee, S. K. S.; VanEgmond, J. W.; Winter, H. H. *Macromolecules* **1999**, *32*, 1167.
(24) Pogodina, N. V.; Winter, H. H. *Macromolecules* **1998**, *31*, 8164.
(25) Devaux, N.; Monasse, B.; Haudin, J. M.; Vermant, J.; Moldenaers, P.; Andre, J. M.; Ernst, B. *Proceedings of the International Conference on Flow Induced Crystallization of Polymers*, Salerno, Italy, 14−17, 2001; p 31.
(26) Jerschow, P.; Janeschitz-Kriegl, H. *Int. Polym. Process.* **1997**, *12*, 72.
(27) Eder, G.; Janeschitz-Kriegl, H.; Liedauer, S. *Prog. Polym. Sci.* **1990**, *15*, 629.
(28) Liedauer, S.; Eder, G.; Janeschitz-Kriegl, H. *Int. Polym. Process.* **1995**.
(29) Kumaraswamy, G.; Kornfield, J. A.; Yeh, F.; Hsiao, B. S. *Macromolecules* **2002**, *35*, 1762.
(30) Kumaraswamy, G.; Varma, R. K.; Issaian; A. M.; Kornfield, J. A.; Yeh, F.; Hsiao, B. S. *Polymer* **2000**, *41*, 8931.
(31) Kumaraswamy, G.; Issaian, A. M.; Kornfield, J. A. *Macromolecules* **1999**, *32*, 7537.
(32) Kumaraswamy, G.; Varma, R. K.; Kornfield, J. A. *Rev. Sci. Instrum.* **1999**, *70*, 2097.

(33) Mitchell, G. R.; Holt, J. J.; Thornley, S. A.; Chai, C. K. *Proceedings of the International Conference on Flow Induced Crystallization of Polymers*, Salerno, Italy, 14−17, 2001; p 15.
(34) Ryan, J.; Terrill, N. J.; Fairclough, J. P. A. In *Scattering of Polymers*; Cebe, P., Hsiao, B. S., Lohse, D. J., Eds.; *ACS Symp. Ser.* **2000**, *739*, 201.
(35) Terrill, N. J.; Fairclough, J. P. A.; Towns-Andrews, E.; Komanschek, B. U.; Young, R. J.; Ryan, A. J. *Polymer* **1998**, *39*, 2381.
(36) Somani, R. H.; Yang, L.; Hsiao, B. S. *Physica A* **2002**, *304*, 145.
(37) Somani, R. H.; Nogales, A.; Srinivas, S.; Fruitwala, H.; Tsou, A. H.; Hsiao, B. S. *Proceedings of the International Conference on Flow Induced Crystallization of Polymers*, Salerno, Italy, 14−17, 2001; p 21.
(38) Somani, R. H.; Bruger, C.; Hsiao, B. S.; Stein, R. S. *Proceedings of ACS Division of Polymeric Materials: Science and Engineering*, Chicago, August 26−30, 2001; Vol. 85, p 429.
(39) Somani, R. H.; Hsiao, B. S.; Nogales, A.; Srinivas, S. Tsou, A. H.; Sics, I.; Balta-Calleja, F.; Ezquerra, T. A. *Macromolecules* **2000**, *33*, 9385.
(40) Nogales, A.; Hsiao, B. S.; Somani, R. H.; Srinivas, S. Tsou, A. H.; Balta-Calleja, F.; Ezquerra, T. A. *Polymer* **2000**, *42*, 5247.
(41) Somani, R. H.; Hsiao, B. S.; Nogales, A.; Srinivas, S.; Tsou, A. H.; Balta-Calleja, F.; Ezquerra, T. A. *Macromolecules* **2001**, *34*, 5902.
(42) Tribout, C.; Monasse, B.; Haudin, J. *Colloid Polym. Sci.* **1996**, *274*, 197.
(43) Monasse, B. *J. Mater. Sci.* **1995**, *30*, 5002.
(44) Duplay, C.; Monasse, B.; Haudin, J.; Costa, J. *Polym. Int.* **1999**, *48*, 320.
(45) Alfonso, G. C.; Azzurri, F. *Proceedings of the International Conference on Flow Induced Crystallization of Polymers*, Salerno, Italy, 14−17, 2001; p 27.
(46) Bassett, D. C., *Proceedings of the International Conference on Flow Induced Crystallization of Polymers*, Salerno, Italy, 14−17, 2001; p 59.
(47) Abo el Maaty, M. I.; Bassett, D. C. *Polymer* **2001**, *42*, 4957.
(48) Abo el Maaty, M. I.; Bassett, D. C. *Polymer* **2001**, *42*, 4965.
(49) Strobl, G. *Eur. Polym. J.* **2000**, *E3*, 165.
(50) Lotz, B. *Eur. Polym. J.* **2000**, *E3*, 185.
(51) Imai, M.; Mori, K.; Mizukami, T.; Kaji, K.; Kanaya, T. *Polymer* **1992**, *33*, 4451.
(52) Imai, M.; Kaji, K.; Kanaya, T.; Sakai, Y. *Phys. Rev. B* **1995**, *52*, 12696.
(53) Imai, M.; Kaji, K.; Kanaya, T. *Macromolecules* **1994**, *27*, 7103.
(54) Petermann, J. *Macromol. Chem. Phys.* **1981**, *182*, 613.
(55) Petermann, J.; Gohil, R. M.; Schultz, J. M.; Hendricks, R. W.; Lin, J. S. *J. Polym. Sci., Polym. Phys.* **1982**, *20*, 523.
(56) Meakin, P.; Scalapino, D. J. *J. Polym. Sci., Polym. Phys.* **1985**, *23*, 179.
(57) Wang, Z. G.; Hsiao, B. S.; Sirota, E.; Agarwal, P.; Srinivas, S. *Macromolecules* **2000**, *33*, 978.
(58) Wang, Z. G.; Hsiao, B. S.; Sirota, E. B.; Srinivas, S. *Polymer* **2000**, *41*, 8825.
(59) Cheng, S. Z. D.; Li, C. Y.; Zhu, L. *Eur. Phys. J. E: Soft Matter* **2000**, *3*, 195.
(60) Liu, C.; Muthukumar, M. *J. Chem. Phys.* **1998**, *109*, 2536.
(61) Muthukumar, M. *Eur. Phys. J. E: Soft Matter* **2000**, *3*, 199.
(62) Samon, J. M.; Schultz, J. M.; Hsiao, B. S.; Seifert, S.; Stribeck, N.; Gurke, , I.; Collins, G.; Saw, C. *Macromolecules* **1999**, *32*, 8121.
(63) Schultz, J. M.; Hsiao, B. S.; Samon, J. M. *Polymer* **2000**, *41*, 8887.
(64) Ran, S.; Zong, X.; Fang, D.; Hsiao, B. S.; Chu, B.; Ross, R. *J. Appl. Crystallogr.* **2000**, *33*, 1031.
(65) Lieberwirth, I.; Loos, J.; Petermann, J.; Keller, A. *J. Polym. Sci., Part B: Polym. Phys.* **2000**, *38*, 1183.
(66) Seki, M.; Thurman, D. W.; Oberhauser, J. P.; Kornfield, J. A. *Macromolecules* **2002**, *35*, 2583.
(67) Pennings, A. J.; Kiel, A. M. *Kolloid Z. Z. Polym.* **1965**, *205*, 160.
(68) Rau, J.; Gohil, R. M.; Petermann, J.; Schultz, J. M. *Colloid Polym. Sci.* **1981**, *259*, 241.

MA020785O